学位論文（要約）

Expression and functional analyses of chromatin remodeling factor Baf60c during heart regeneration

(心臓再生過程におけるクロマチンリモデリング因子 Baf60c の発現および機能解析)

平成 27 年 12 月博士（理学）申請

東京大学大学院理学系研究科

生物科学専攻

中村　遼

Contents

Abbreviations

- *α-MHC* *Alpha-myosin heavy chain*
- Baf60c BRG1/BRM-associated factor 60c
- Brg1 Brahma (BRM)-related gene 1 (Brg1/Brm)
- ChIP Chromatin immunoprecipitation
- cTnT Cardiac troponin T
- dpr Days post resection
- E Embryonic day
- GFP Green fluorescent protein
- H3K4me1 Histone H3 Lys4 monomethylation
- H3K4me3 Histone H3 Lys4 trimethylation
- H3K27ac Histone H3 Lys27 acetylation
- H3K27me3 Histone H3 Lys27 trimethylation
- MI Myocardial infarction
- P Postnatal day
- PHH3 Phospho-histone H3
- Pol II RNA polymerase II
- qRT-PCR Quantitative reverse transcription-polymerase chain reaction
- SWI/SNF SWItch/Sucrose Non-Fermentable chromatin remodeling complex
- tg Transgenic
- TSS Transcription start site
- wt Wild type

第１章の一部および第２章の一部を５年以内に雑誌等で刊行予定のため、非公開。

第１章の一部および第２章の一部を５年以内に雑誌等で刊行予定のため、非公開。

第１章の一部および第２章の一部を５年以内に雑誌等で刊行予定のため、非公開。

第１章の一部および第２章の一部を５年以内に雑誌等で刊行予定のため、非公開。

第１章の一部および第２章の一部を５年以内に雑誌等で刊行予定のため、非公開。

第１章の一部および第２章の一部を５年以内に雑誌等で刊行予定のため、非公開。

第１章の一部および第２章の一部を５年以内に雑誌等で刊行予定のため、非公開。

Chapter I

Analysis of Baf60c during mouse heart development

第 1 章

本章については、一部を 5 年以内に雑誌等で刊行予定のため、非公開。

第 1 章

本章については、一部を 5 年以内に雑誌等で刊行予定のため、非公開。

第 1 章

本章については、一部を 5 年以内に雑誌等で刊行予定のため、非公開。

第１章

本章については、一部を５年以内に雑誌等で刊行予定のため、非公開。

第１章

本章については、一部を５年以内に雑誌等で刊行予定のため、非公開。

Results

Expression analysis of Baf60c during mouse heart development

Smarcd3 is highly expressed in embryonic mouse hearts

Baf60c plays a critical role in cardiac differentiation and proliferation at early embryonic stages (Lickert *et al.* 2004; Takeuchi and Bruneau 2009). Previous studies showed that Baf60c is expressed very early in the precardiac mesoderm, late gastrulation, and prenodal plate stages. At later stages, the expression of Baf60c becomes restricted to the regions of heart, somite, and central nervous system (Debril *et al.* 2004; Lickert *et al.* 2004). However, it is unclear whether Baf60c is expressed and functions after cardiac maturation. To know this, I examined the expression of Baf60c during cardiac maturation *in vivo*. I first performed *in situ* hybridization in developing mouse hearts. An intense signal of *Smarcd3*, which encodes Baf60c, was detected in the entire heart at early developmental stages as same as Lickert *et al.* (2004) (Figure 1A, E 8.0 and E9.5). After birth, in P0 and 13-week-old (13 weeks) mice, the signal was nearly undetectable in the ventricles (Figure 1A, P0 and 13 weeks).

Next I examined the mRNA expression levels of all three Baf60c variants, *Smarcd1* (Baf60a), *Smarcd2* (Baf60b), and *Smarcd3* (Baf60c) (Figure 2; Ho and Crabtree 2010), to determine which variant was associated with heart development. To do that, I quantified the expression levels of all three *Smarcds* mRNA by qRT-PCR with mouse ventricles at several developmental stages (Figure 1B). *Smarcd3* showed a

reduction in expression levels during heart development. The expression of *Smarcd3* was high in the E9.5 ventricle, whereas it was decreased by P26. On the other hand, *Smarcd1* and *Smarcd2* formed the expression peaks at P7, these peaks were later than that of *Smarcd3*. There were some differences in *Smarcd3* expression between *in situ* hybridization and qRT-PCR analysis. In the qRT-PCR data, the expression level of *Smarcd3* in the P7 ventricle was nearly the same as that was observed in the embryo. On the other hands, in the *in situ* hybridization data, the expression of *Smarcd3* was hardly detectable in the ventricles after birth. *In situ* hybridization was suitable for detecting the signal, which was observed in a restricted region. Thus, I supposed that *Smarcd3* was expressed in the ventricle but its expression level could be variable after birth.

第１章

本章については、一部を５年以内に雑誌等で刊行予定のため、非公開。

第 1 章

本章については、一部を 5 年以内に雑誌等で刊行予定のため、非公開。

第１章

本章については、一部を５年以内に雑誌等で刊行予定のため、非公開。

第１章

本章については、一部を５年以内に雑誌等で刊行予定のため、非公開。

第１章

本章については、一部を５年以内に雑誌等で刊行予定のため、非公開。

第１章

本章については、一部を５年以内に雑誌等で刊行予定のため、非公開。

第 1 章

本章については、一部を 5 年以内に雑誌等で刊行予定のため、非公開。

Chapter II

Analysis of Baf60c during heart regeneration in neonatal mice and axolotls

第 2 章

本章については、一部を 5 年以内に雑誌等で刊行予定のため、非公開。

第 2 章

本章については、一部を 5 年以内に雑誌等で刊行予定のため、非公開。

第 2 章

本章については、一部を 5 年以内に雑誌等で刊行予定のため、非公開。

第 2 章

本章については、一部を 5 年以内に雑誌等で刊行予定のため、非公開。

第 2 章

本章については、一部を 5 年以内に雑誌等で刊行予定のため、非公開。

第 2 章

本章については、一部を５年以内に雑誌等で刊行予定のため、非公開。

第 2 章

本章については、一部を 5 年以内に雑誌等で刊行予定のため、非公開。

Results

Expression analysis of Baf60c during heart regeneration in neonatal mice

Cell proliferation in the regenerating neonatal mouse hearts

Two mouse models are used to study cardiac regeneration; Myocardial infarction (MI) and cardiac resection. The cardiac resection is experimentally easier and more controllable in animals that exhibit strong regenerative abilities, such as zebrafish and neonatal mice (Poss *et al.* 2002; Porrello *et al.* 2011; Mahmoud *et al.* 2014). I therefore adopted the cardiac resection in my study to elucidate the regeneration mechanism in neonatal mice and axolotls. Neonatal mice exhibit heart regeneration after resection, but this capacity is lost by P7 (Porrello *et al.* 2011). To clarify the interaction between Baf60c and cell proliferation in heart regeneration, I performed apical ventricular resection in neonatal mouse (Figure 6). Immunofluorescence staining revealed ectopic cell proliferation in the neonatal mouse hearts following resection (Figure 7A, B). Cardiac troponin T (cTnT) is a cardiac-specific sarcomere factor, and then I identified cardiomyocytes as cTnT-positive cells. Mitotic cells were labeled with anti-Ki67 antibody. The Ki67-positive cardiomyocytes were observed at 2 days post-resection (dpr) in both the border region (Figure 7Aa) and the apical region (Figure 7Ab). At 8 dpr, there were several Ki67-positive cardiomyocytes near the border region (Figure 7B), but at 22 dpr, when the lost tissue was almost completely regenerated, I could not

detect Ki67-positive cells (Figure 7C). These results indicated that the cardiomyocyte proliferation occurred rapidly and was completely downregulated by 22 dpr.

Baf60c staining in the regenerating neonatal mouse hearts

As robust cardiomyocyte proliferation was observed at 2 dpr, I examined Baf60c expression over this time period to determine the relationship between Baf60c and cell proliferation in the regenerating heart. Strong Baf60c expression was observed in the cells surrounding the resected plane at 2 dpr (Figure 8A, C), but its expression was weak in the remote regions of both resected and sham-operated ventricles (Figure 8B, D, E). In general, Baf60c is thought to be a nucleoprotein, but I detected Baf60c in both nuclei and cytoplasm near the resected plane (Figure 8C). In the remote region of both resected ventricle and sham-operated ventricle, Baf60c protein was localized to the cell nuclei (Figure 8D, E). Near the resected plane several Baf60c staining was observed in the cardiomyocytes (Figure 8F), while in the remote region of both resected and sham-operated ventricles, only a few number of Baf60c signals were detected in the cardiomyocytes (Figure 8G, H). This result suggests that a small number of Baf60c-positive cardiomyocytes exist in the ventricle of the newborn mouse heart and Baf60c-positive cardiomyocytes are increased near the resected plane after resection. As strong Baf60c expression was observed in the injured apical region (Figure 8C), where scar tissue was present instead of cardiomyocytes, I examined the co-localization of Baf60c and fibroblasts, a major component of scar tissue. To label the fibroblasts, I utilized the anti-vimentin antibody. After resection, the number of vimentin-positive

fibroblasts were increased near the resected plane, and I found that Baf60c signals were co-localized with vimentin-positive fibroblasts in the injured apical region (Figure 8I). This result indicates that the Baf60c-positive fibroblasts were induced in the injury site following resection. Interestingly in the remote region, Baf60c, cTnT, and vimentin triple positive cells were observed (Figure 8G, H, J, K).

Gene expression pattern in the neonatal mouse during heart regeneration

I quantified the mRNA expression levels of several cardiac factors during neonatal mouse heart regeneration. *Smarcd3* (Baf60c) was upregulated in the resected ventricle at 3 and 5 dpr compared to the sham-operated ventricles (Figure 9A). At 1 dpr, *Smarcd3* expression was downregulated compared to the sham-operated ventricles, suggesting that Baf60c induction could be regulated by other factors, such as inflammatory response genes, which respond immediately following injury. The expression levels of *Smarca4*, which encodes Brg1, and *Gata4* were constant by 5 dpr (Figure 9B, C). The expression of *Tnnt2,* which encodes cTnT, was strongly decreased at 1 dpr and then increased at 3 dpr (Figure 9D).

As Baf60c upregulation was observed in cardiomyocyte after resection (Figure 8F), I next examined gene expression patterns in cardiomyocytes near the apical region of ventricle during neonatal mouse heart regeneration. I identified cardiomyocytes as *α-MHC*-positive cells. To collect *α-MHC*-positive cells, I used *α-MHC-GFP*-tg mice, in which GFP is driven by an *α-MHC* promoter. Therefore, *α-MHC*-positive cells can be isolated as GFP-positive cells using flow cytometry

(Figure 10A). As a result of qRT-PCR, a reduction of *Smarcd3* expression at 3 dpr and upregulation at 5 dpr compared to the sham-operated ventricle were observed (Figure 10Ba). Interestingly, the expression of *Smarca4* (Brg1) was significantly upregulated in the resected heart at 5 and 8 dpr (Figure 10Ba). The upregulation of both *Smarcd3* and *Smarca4* suggested that the expression and function of the SWI/SNF-BAF complex in cardiomyocytes could be stimulated in response to cardiac stress. Several embryonic cardiac transcription factors, such as *Gata4*, *Nkx2.5*, and *Mef2c*, were also upregulated post-resection (Figure 10Bb), suggesting that these transcription factors interact with SWI/SNF complex during heart regeneration, similar to their function during heart development. On the other hand, the expression of *Tbx5* was significantly downregulated at 3 and 8 dpr (Figure 10Bb). The expressions of sarcomere genes, such as *Tnnt2* and *Tnni3*, were increased in resected cardiomyocytes at 5 dpr after the upregulation of transcription factors (Figure 10Bc), suggesting that these sarcomere genes were regulated by cardiac transcription factors as cardiomyocyte differentiation.

Knockdown experiments of Baf60c during heart regeneration in neonatal mice

A lack of cell proliferation in the si*Smarcd3*-transfected cardiomyocytes *in vitro*

My previous results showed that the cardiomyocyte proliferation and the upreguation of Baf60c occurred after heart resection in neonatal mouse (Figure 7-10). Furthermore, it was already reported that cardiomyocyte proliferation is required for heart regeneration following injury (Poss *et al.*, 2002; Jopling *et al.*, 2010; Kikuchi *et al.*, 2010; Porrello *et al.*, 2011). To reveal whether Baf60c has an effect on cardiomyocyte proliferation, I

performed a knockdown experiment by transfecting siRNA against *Smarcd3* (si*Smarcd3*) into cultured cardiomyocytes (Figure 11A). To collect the cardiomyocytes, I isolated the *α-MHC*-positive cells from *α-MHC-GFP*-tg mice using flow cytometry. The isolated cardiomyocytes were cultured on feeder cells and transfected with siRNA. When the cardiomyocytes were treated with si*Smarcd3*, the expression of *Smarcd3* was specifically repressed, typically achieving 90% knockdown with minimal off-target effects (Figure 12). After 72 h, the cells were fixed with 4% paraformaldehyde in PBS for co-staining with anti-cTnT and anti-Ki67 antibodies (Figure 11B). I performed siRNA transfection in two types of cultured cells: postnatal *α-MHC*-positive cells (Figure 11C) and *α-MHC*-positive cells at 1 dpr (Figure 11D). In both types of cultured cells, the number of proliferating cardiomyocytes (both cTnT-positive and Ki67-positive cells) treated with si*Smarcd3* was reduced by more than one third compared with the control condition (Figure 11C, D). These data suggested that Baf60c played an important role in cardiomyocyte proliferation in the postnatal heart and also in the regenerating heart.

第 2 章

本章については、一部を５年以内に雑誌等で刊行予定のため、非公開。

第 2 章

本章については、一部を 5 年以内に雑誌等で刊行予定のため、非公開。

第 2 章

本章については、一部を 5 年以内に雑誌等で刊行予定のため、非公開。

第 2 章

本章については、一部を 5 年以内に雑誌等で刊行予定のため、非公開。

第 2 章

本章については、一部を 5 年以内に雑誌等で刊行予定のため、非公開。

第 2 章

本章については、一部を 5 年以内に雑誌等で刊行予定のため、非公開。

Expression analysis of Baf60c during heart regeneration in axolotls

Histology and cell proliferation in axolotl during heart regeneration

My previous data showed that cardiomyocyte proliferation and Baf60c upregulation occurred as the same time course during heart regeneration in neonatal mice. To test whether such phenomenon was conserved in other regenerative animals, I performed the apical resection surgery on axolotls. As axolotls have high regenerative capacity through their life, regeneration studies using limbs and tails have been frequently carried out; however, less is known about heart regeneration. Therefore, I first studied the process of the axolotl heart regeneration. In the axolotl, it took almost 3 weeks to regenerate the heart, and the heart morphology near the resected surface at 24 dpr seemed to be completely regenerated (Figure 21A, B). Unlike other regenerative animals such as zebrafish and neonatal mice, no fibrotic scar was observed near the resected surface following resection (Figure 21B).

To address whether cell proliferation occurred following injury, I performed immunofluorescence staining using an anti-pHH3 antibody on the axolotl heart sections. Mitotic cells were labeled with anti-phospho-histone H3 (pHH3) antibody. Interestingly the pHH3-positive cells were widely detected in the axolotl ventricle 2 dpr (Figure 22A), and the number of pHH3-positive cells in the ventricle rapidly decreased at 9, 15, and 24 dpr (Figure 22A, B). These data suggested that cell proliferation occurred in the entire region of the ventricle and induced immediately following cardiac resection in axolotl as well as neonatal mice.

Upregulation of Baf60c in the axolotl during heart regeneration

Next, I performed Western blotting analysis to determine whether Baf60c was expressed in the axolotl heart regeneration. As the widespread cell proliferation occurred at early stage in the axolotl heart regeneration, I analyzed Baf60c expression in this time period. The ventricles of the axolotl heart at 3 dpr showed intense Baf60c expression near the resected surface (apex) and also in the remote region of the injury, although Baf60c was less expressed in the sham-operated ventricles and intact ventricles (denoted as 'Not operated' in Figure 23) (Figure 23). Baf60c upregulation in the entire ventricle after resection was consistent with the widespread cell proliferation. These data suggested that the interaction between Baf60c upregulation and cell proliferation in regenerating hearts was conserved in both axolotls and neonatal mice.

第 2 章

本章については、一部を 5 年以内に雑誌等で刊行予定のため、非公開。

第 2 章

本章については、一部を 5 年以内に雑誌等で刊行予定のため、非公開。

第 2 章

本章については、一部を 5 年以内に雑誌等で刊行予定のため、非公開。

第 2 章

本章については、一部を 5 年以内に雑誌等で刊行予定のため、非公開。

第 2 章

本章については、一部を 5 年以内に雑誌等で刊行予定のため、非公開。

第 2 章

本章については、一部を 5 年以内に雑誌等で刊行予定のため、非公開。

第 2 章

本章については、一部を 5 年以内に雑誌等で刊行予定のため、非公開。

第 2 章

本章については、一部を 5 年以内に雑誌等で刊行予定のため、非公開。

第 2 章

本章については、一部を 5 年以内に雑誌等で刊行予定のため、非公開。

第１章の一部および第２章の一部を５年以内に雑誌等で刊行予定のため、非公開。

第１章の一部および第２章の一部を５年以内に雑誌等で刊行予定のため、非公開。

第１章の一部および第２章の一部を５年以内に雑誌等で刊行予定のため、非公開。

第１章の一部および第２章の一部を５年以内に雑誌等で刊行予定のため、非公開。

第１章の一部および第２章の一部を５年以内に雑誌等で刊行予定のため、非公開。

Figures

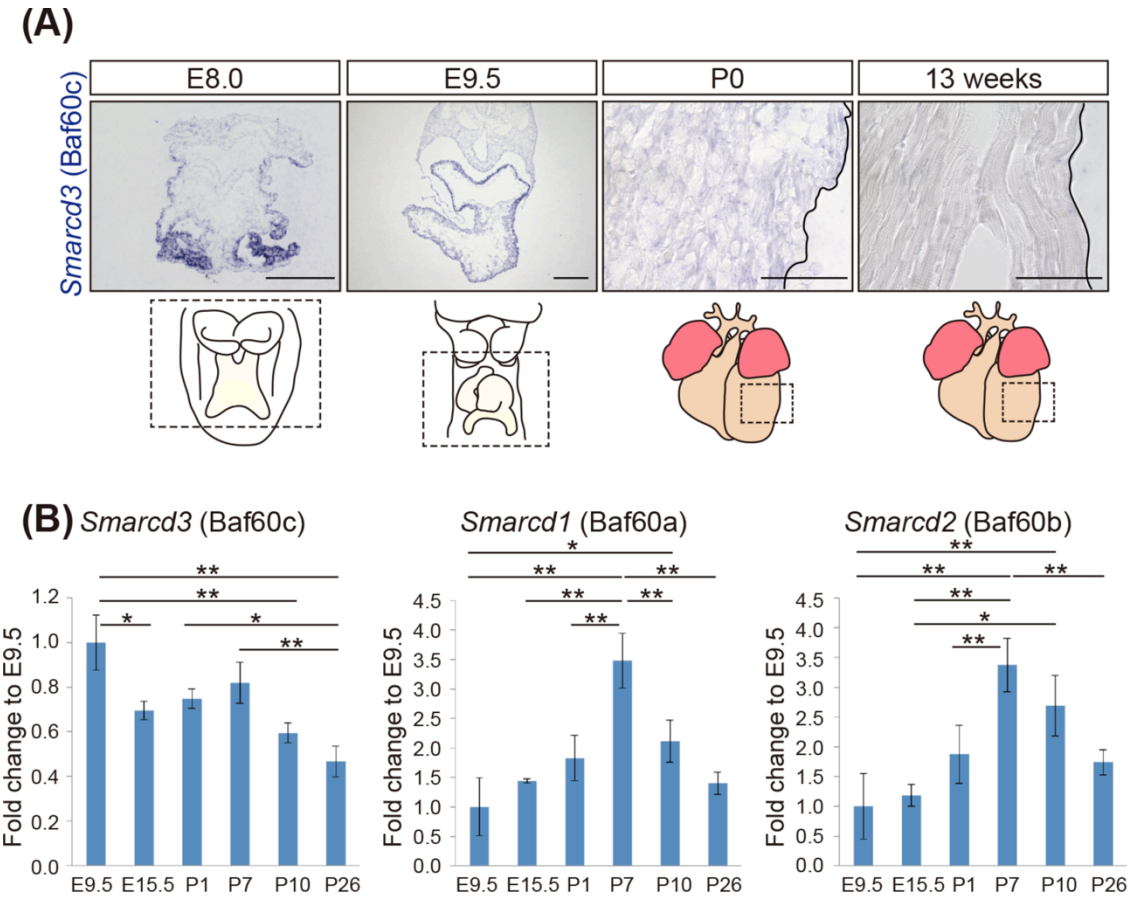

Figure 1. Expression patterns of *Smarcd3* (Baf60c) in mouse heart development.

(A) *In situ* hybridization images of embryo and heart sections from E8.0, E9.5, P0, and 13 weeks mice. Strong *Smarcd3* expression was detected in E8.0 and E9.5 entire hearts. The solid lines at P0 and 13 weeks indicate the edge of the ventricle. The scale bars at E8.0 and E9.5 represent 200 μm, and those at P0 and 13 weeks represent 50 μm. Illustrations indicate the relative regions of *in situ* hybridization images.

(B) mRNA expression levels of *Smarcd3* (Baf60c), *Smarcd1* (Baf60a), and *Smarcd2* (Baf60b) in ventricles during mouse heart development. The expression of *Smarcd3* (Baf60c) is high at embryonic stages and reduced following cardiac maturation. The error bars represent the mean ± s.d. The *P-values* are evaluated using Tukey's honestly significant difference test and Bonferroni corrections; n=3 per group; *$P<0.05$, ** $P<0.01$.

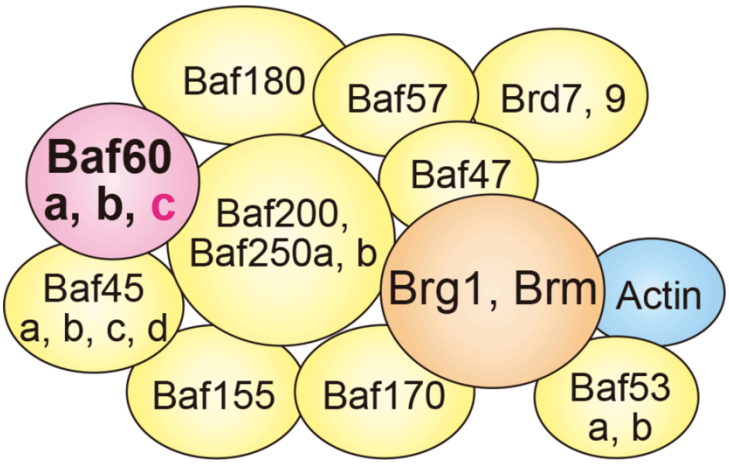

Figure 2. A schematic diagram of the mammalian SWI/SNF-BAF complex.

The SWI/SNF-BAF complex remodels chromatin conformation by recruiting Pol II. There are three Baf60 variants, Baf60a, Baf60b, and Baf60c. The complex contains either of two ATPase subunits, Brg1 or Brm as a core factor for its function.

第１章の一部を５年以内に雑誌等で刊行予定のため、非公開。

第 1 章の一部を 5 年以内に雑誌等で刊行予定のため、非公開。

第 1 章の一部を 5 年以内に雑誌等で刊行予定のため、非公開。

第 1 章の一部を 5 年以内に雑誌等で刊行予定のため、非公開。

第 1 章の一部を 5 年以内に雑誌等で刊行予定のため、非公開。

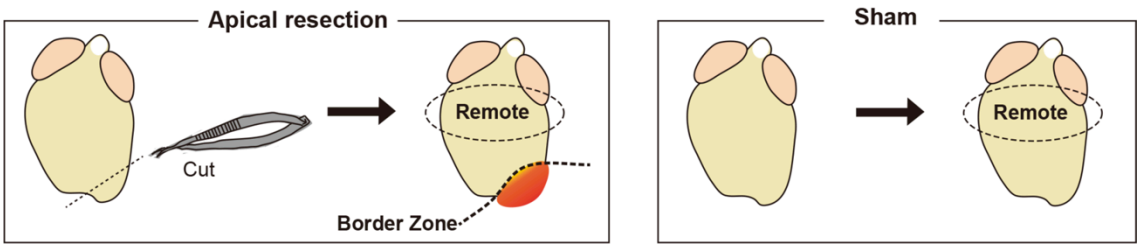

Figure 6. **Apical resection surgery in neonatal mouse heart.**

Schematic diagram of apical resection, sham-operation, and the regions for observation in Figures 7 and 8.

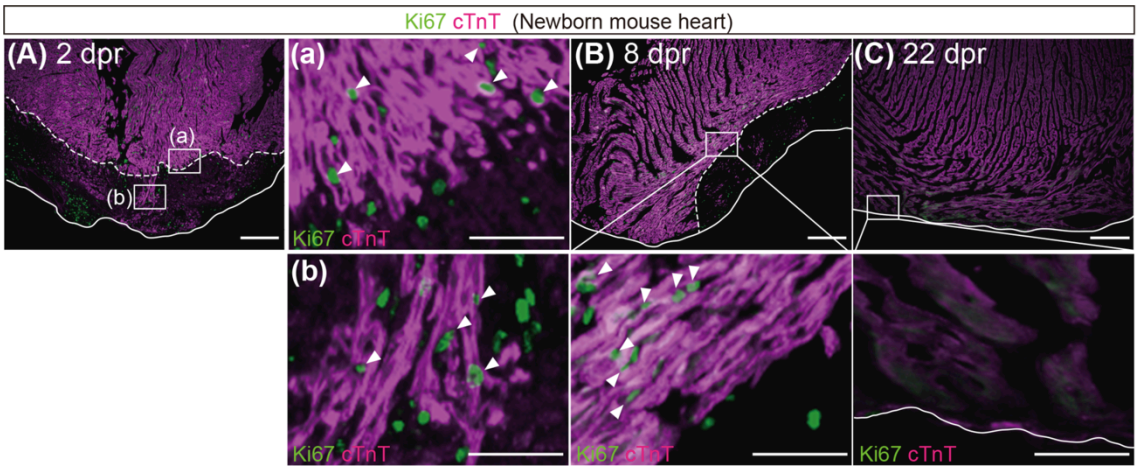

Figure 7. **Cardiomyocyte proliferation in the regenerating neonatal mouse heart.** (A-C) Cardioimyocyte proliferation in regenerating neonatal mouse hearts. Co-staining of Ki67 (green) and cardiac troponin T (cTnT, magenta) in the postnatal mouse hearts at 2 dpr (A), 8 dpr (B), and 22 dpr (C). Mitotic cells are labeled with anti-Ki67. The boxed areas in (A) are magnified in the right panels (marked as [a] and [b]). The boxed areas in (B) and (C) are magnified in each bottom panels. The white arrowheads indicate cTnT-positive and Ki67-positive cardiomyocytes. The dashed lines indicate the resected plane. The solid lines indicate the edge of ventricle. The scale bars in the low-magnification panels represent 200 μm; in the high-magnification panels, the bars represent 50 μm.

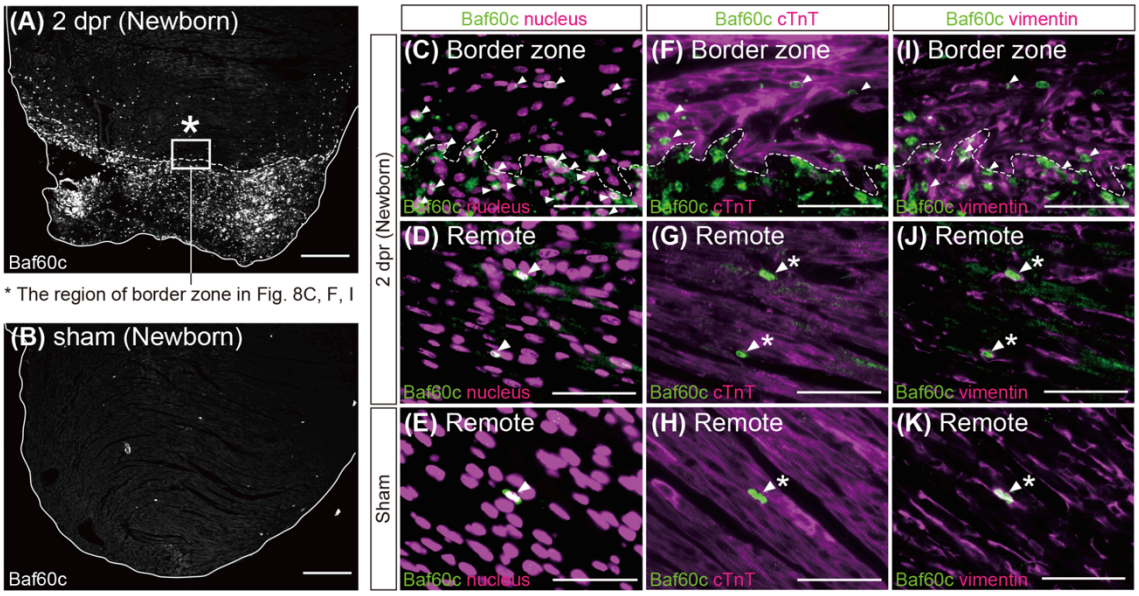

Figure 8. Baf60c expression in the regenerating neonatal mouse heart post-resection and sham-operated heart.

(A, B) Low magnification images of Baf60c show intense signal in the apical region of neonatal mouse ventricle at 2 dpr (A) and weak signal in sham-operated ventricle (B). The box area in (A) represents the border zone (marked as *) and is magnified in the panels in (C, F, I). The dashed line indicates the resected plane. The solid lines indicate the edge of ventricle. The scale bars represent 200 μm.

(C-E) The expression patterns of Baf60c (green) and DAPI (nucleus, magenta) in neonatal mouse heart at 2 dpr (C, D) and in sham-operated ventricle (E). (C) is the image of border zone, and (D) and (E) are the images of remote regions. A large number of Baf60c signals are detected near the resected plane (C). The white arrowheads indicate Baf60c which is localized in nuclei.

(F-H) The expression patterns of Baf60c (green) and cTnT (magenta) in the same regions of C-E respectively. Several Baf60c signals are observed in cTnT-positive cardiomyocytes near the resected plane (white arrowheads in F), and a few in the remote region of resected (G) and sham-operated (H) hearts.

(I-K) The expression patterns of Baf60c (green) and vimentin (magenta) in the same regions of C-E respectively. Several Baf60c signals are co-localized in vimentin-positive fibroblasts near the resected plane (white arrowheads in I), and a few in the remote region of resected (J) and sham-operated (K) hearts.

The dashed lines indicate the resected plane. The arrowheads with * indicate Baf60c, cTnT, and vimentin triple positive cells. The scale bars represent 50 μm in (C-K).

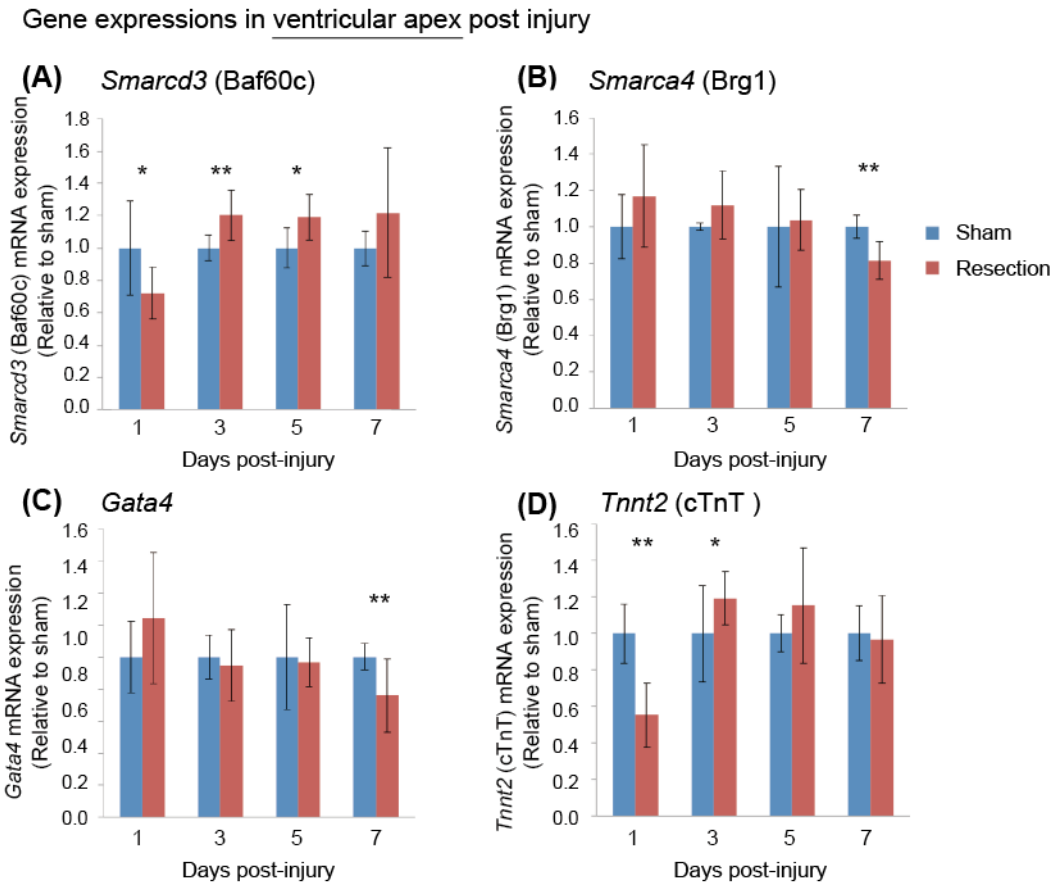

Figure 9. Gene expression patterns in ventricular apex during heart regeneration in neonatal mice.

(A-D) mRNA expression levels of *Smarcd3* (Baf60c), *Smarca4* (Brg1), *Gata4* and *Tnnt2* (cTnT) at 1, 3, 5, and 7 days post-injury (red bars) relative to sham-operated ventricles (blue bars). The values are represented as the mean ± s.d. The *P values* are determined using a two-tailed T-test; n=3 per group; **P*<0.05, ** *P* <0.01.

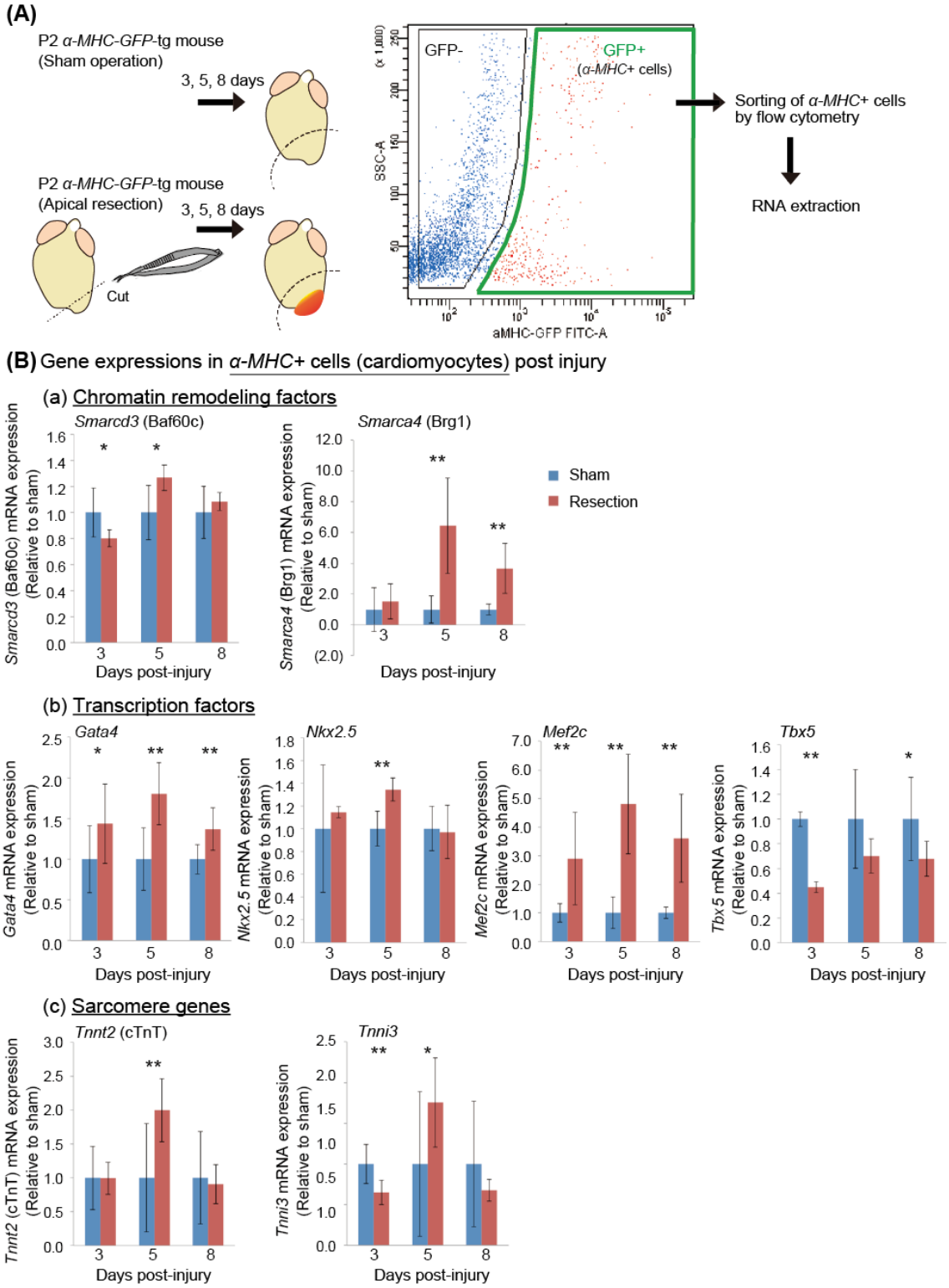

Figure 10. Gene expression patterns in cardiomyocytes during heart regeneration in neonatal mice.

(A) A schematic diagram of collection of cardiomyocytes from sham-operated and resected hearts. *α-MHC*-positive (*α-MHC*+) cells were considered as cardiomyocytes.
(B) mRNA expression levels of chromatin remodeling factors (*Smarcd3* [Baf60c], *Smarca4* [Brg1]), cardiac-specific transcription factors (*Gata4*, *Nkx2.5*, *Mef2c*, *Tbx5*), and sarcomere genes (*Tnnt2* [cTnT], *Tnni3*) at 3, 5, 8 days post-injury (red bars) relative to sham-operated cardiomyocytes (blue bars). The error bars represent the mean ± s.d. The *P values* are determined using a two-tailed T-test; n=3 per group; **P*<0.05, ***P*<0.01.

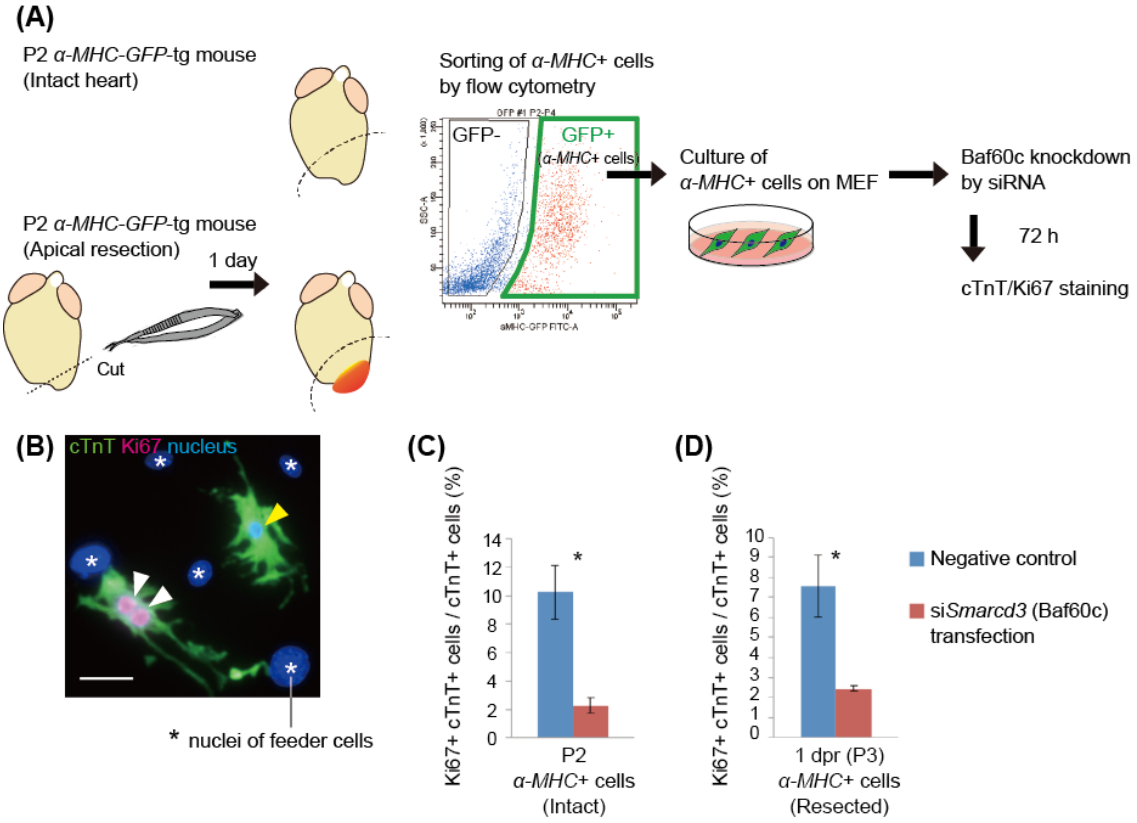

Figure 11. Lack of cardiomyocyte proliferation in the si*Smarcd3*-transfected cells.

(A) A schematic diagram of culture of cardiomyocytes and siRNA treatment.

(B) Image of cTnT (green)/Ki67 (magenta)/DAPI (nucleus, blue) staining. The white arrowheads indicate proliferating cardiomyocytes (Ki67-positive [+] and cTnT-positive [+]). The yellow arrowhead indicates a non-proliferating cardiomyocytes (Ki67-negative [-] and cTnT-positive [+]). * indicate nuclei of feeder cells. The scale bar represents 50 μm.

(C, D) The quantification of proliferating cardiomyocytes relative to cardiomyocytes in the cultured P2 *α-MHC* positive (*α-MHC*+) cells (C) and 1 dpr *α-MHC*+ cells (D). The blue bars (control) represent the data of the transfection of RNAi Negative Control Duplex. The red bars represent the data of the si*Smarcd3*-transfected cardiomyocytes. The number of proliferating cardiomyocytes (Ki67+ cTnT+) is reduced in the si*Smarcd3*-transfected cells. The error bars represent the mean ± s.d. The *P values* are determined using a two-tailed T-test; n=3 per group; *$P<0.05$.

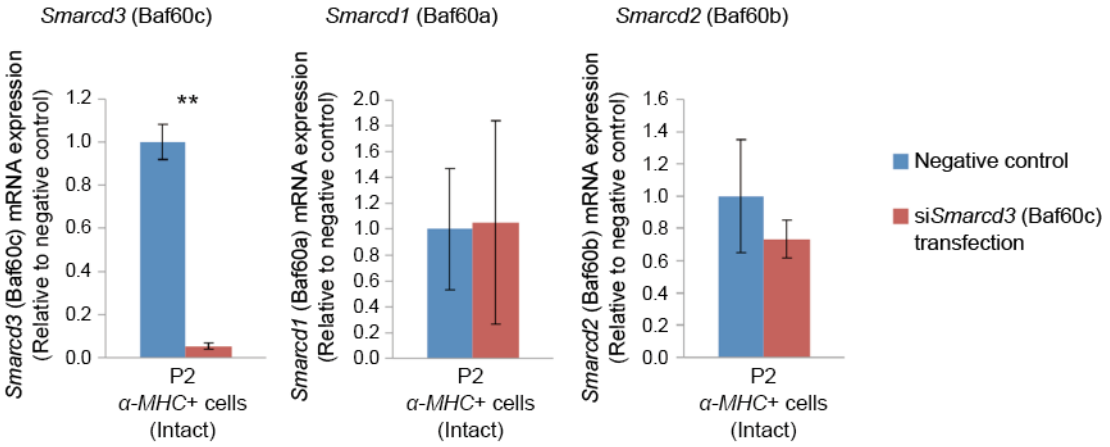

Figure 12. Baf60c-knockdown efficiency by siRNA in the cultured cardiomyocytes from neonatal mice.

mRNA expression levels of *Smarcd3* (Baf60c), *Smarcd1* (Baf60a), and *Smarcd2* (Baf60b) in the si*Smarcd3*-transfected cardiomyocytes (red bars) relative to control (blue bars). The blue bars (control) represent the data of the transfection of RNAi Negative Control Duplex. The error bars represent the mean ± s.d. The *P values* are determined using a two-tailed T-test; n=3 per group; ***P*<0.01.

第２章の一部を５年以内に雑誌等で刊行予定のため、非公開。

第２章の一部を５年以内に雑誌等で刊行予定のため、非公開。

第２章の一部を５年以内に雑誌等で刊行予定のため、非公開。

第２章の一部を５年以内に雑誌等で刊行予定のため、非公開。

第２章の一部を５年以内に雑誌等で刊行予定のため、非公開。

第２章の一部を５年以内に雑誌等で刊行予定のため、非公開。

第２章の一部を５年以内に雑誌等で刊行予定のため、非公開。

第２章の一部を５年以内に雑誌等で刊行予定のため、非公開。

第２章の一部を５年以内に雑誌等で刊行予定のため、非公開。

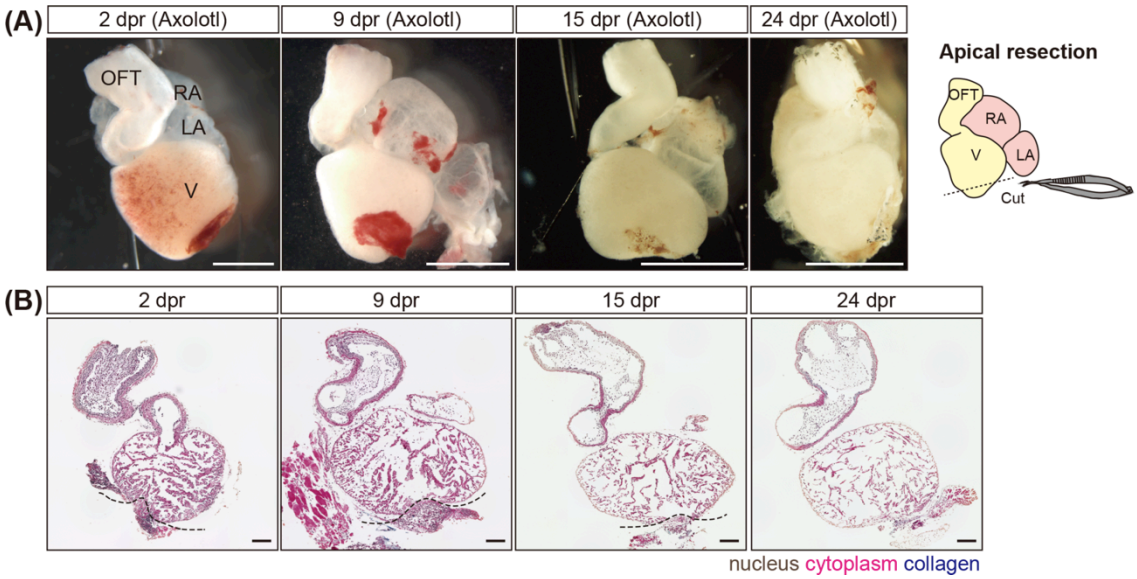

Figure 21. Regeneration in the axolotl heart post-resection.

(A) Bright field images of axolotl hearts at 2, 9, 15, and 24 dpr. RA, right atrium; LA, left atrium; OFT, outflow tract; V, ventricle. The scale bars represent 3 mm.

(B) Masson trichrome staining of the axolotl hearts at 2, 9, 15, and 24 dpr. The heart sections are stained with iron-hematoxylin for nucleus (brown), fuchsine acid for cytoplasm (red), and aniline blue for collagen (blue). Note that blue signals are very weak in the regenerating axolotl heart. The dashed line indicates the resected plane. The scale bars represent 200 μm.

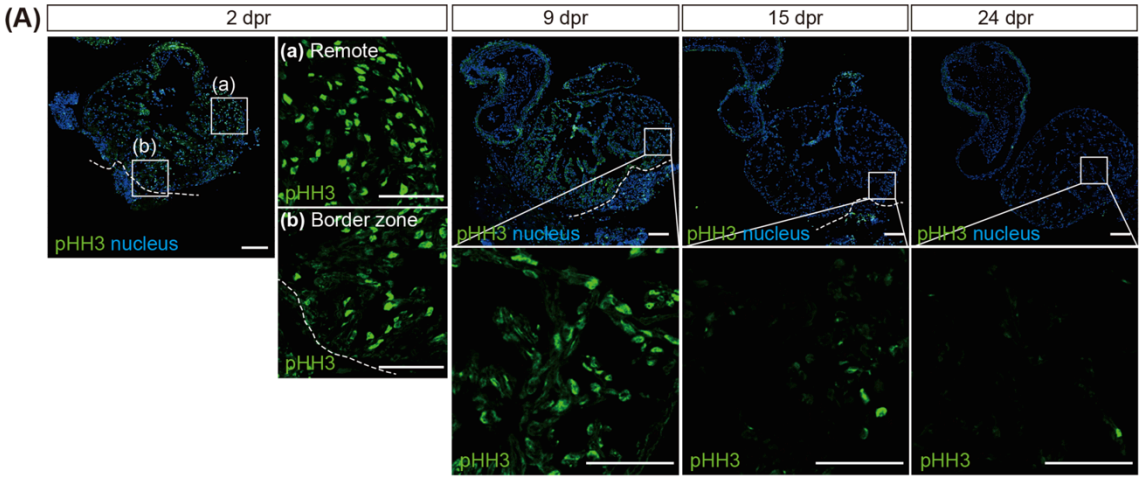

(B)

	2 dpr	9 dpr	15 dpr	24 dpr
Number of pHH3+ cells in ventricle per section	441	58	39	30

Figure 22. Time course of cell proliferation in the axolotl heart regeneration.

(A) Cell proliferation in the regenerating axolotl heart. The mitotic cells are labeled with an anti-pHH3 antibody in axolotl hearts. Staining of pHH3 (green)/DAPI (nucleus, blue) in the axolotl hearts at 2, 9, 15, and 24 dpr. The dashed lines indicate the resected plane. In the 2 dpr section, the boxed areas in the left panel are magnified in the right panels (marked as [a] and [b]). In the sections from 9, 15, and 24 dpr hearts, the boxed areas in the upper panels are magnified in the bottom panels. The scale bars in the low-magnification panels represent 200 μm; in the high-magnification panels, the bars represent 100 μm.

(B) Number of pHH3-positive cells in ventricle per section. Proliferating cells are increased at 2 dpr and decreased by 9 dpr.

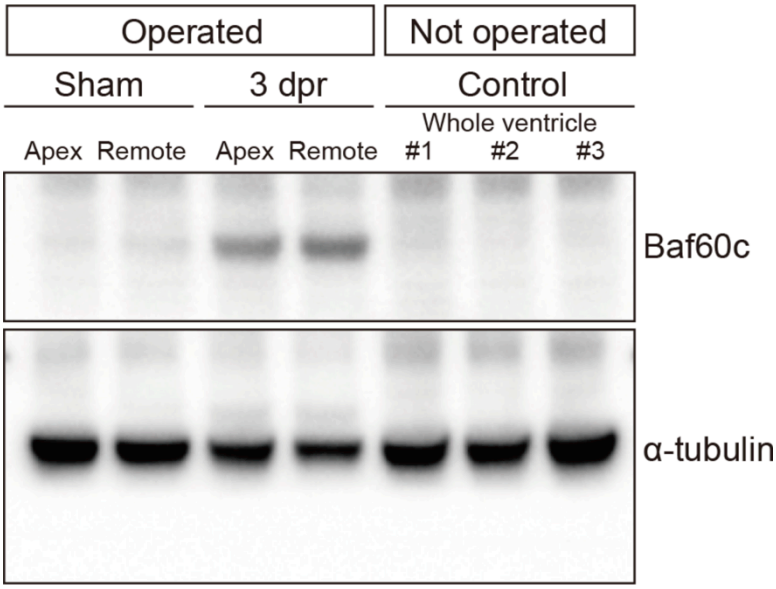

Figure 23. Baf60c upregulation in the axolotl heart regeneration.

Western blotting analysis of axolotl ventricle tissue with anti-Baf60c and anti-α-tubulin antibodies. The two lanes on the left show the results for sham-operated ventricles. The next two lanes show the result for ventricles at 3 dpr. The three right lanes show the results for intact (not operated) ventricles. α-tubulin is utilized as an internal control. Apex: the tip of the ventricle, including the resected plane; Remote: the remote region from the resected plane of the ventricle.

第１章の一部および第２章の一部を５年以内に雑誌等で刊行予定のため、非公開。

第１章の一部および第２章の一部を５年以内に雑誌等で刊行予定のため、非公開。

第１章の一部および第２章の一部を５年以内に雑誌等で刊行予定のため、非公開。

第１章の一部および第２章の一部を５年以内に雑誌等で刊行予定のため、非公開。

第１章の一部および第２章の一部を５年以内に雑誌等で刊行予定のため、非公開。

第１章の一部および第２章の一部を５年以内に雑誌等で刊行予定のため、非公開。

第１章の一部および第２章の一部を５年以内に雑誌等で刊行予定のため、非公開。

第１章の一部および第２章の一部を５年以内に雑誌等で刊行予定のため、非公開。

第１章の一部および第２章の一部を５年以内に雑誌等で刊行予定のため、非公開。

第１章の一部および第２章の一部を５年以内に雑誌等で刊行予定のため、非公開。

第１章の一部および第２章の一部を５年以内に雑誌等で刊行予定のため、非公開。

第１章の一部および第２章の一部を５年以内に雑誌等で刊行予定のため、非公開。

第１章の一部および第２章の一部を５年以内に雑誌等で刊行予定のため、非公開。

第１章の一部および第２章の一部を５年以内に雑誌等で刊行予定のため、非公開。

第１章の一部および第２章の一部を５年以内に雑誌等で刊行予定のため、非公開。

第１章の一部および第２章の一部を５年以内に雑誌等で刊行予定のため、非公開。